JOURNAL OF SOLID STATE CHEMISTRY 3, 174–179 (1971)

Structure and Properties of the High and Low Pressure Forms of $SrIrO_3$*

J. M. LONGO†, J. A. KAFALAS, AND R. J. ARNOTT‡

Lincoln Laboratory, Massachusetts Institute of Technology, Lexington, Massachusetts 02173

Received September 18, 1970

The structure of the atmospheric pressure form of $SrIrO_3$ is shown to be a monoclinic distortion of the hexagonal $BaTiO_3$ structure ($a = 5.604$ Å, $b = 9.618$ Å, $c = 14.17$ Å, $\beta = 93.26°$). The cell dimensions have been studied to 1000°C and the coefficients of thermal expansion given. The structure transforms at 40 kbar and 1000°C to an orthorhombic perovskite ($a = 5.60$ Å, $b = 5.58$ Å, $c = 7.89$ Å) with a 3% decrease in volume. This high pressure phase only retransforms slowly at atmospheric pressure and 1200°C and exhibits metallic conductivity and Pauli paramagnetism.

The compound $SrIrO_3$ can be prepared at atmospheric pressure by the equimolar reaction of $SrCO_3$ and IrO_2 or Ir at 900°C for 20 hr. Rodi (*1*) reported the formation of this compound but did not successfully index the powder pattern. We have found that the X-ray powder pattern can be completely indexed using a monoclinic (*m*) unit cell ($a = 5.604$ Å, $b = 9.618$ Å, $c = 14.17$ Å, $\beta = 93.26°$) which is closely related to a hexagonal (*h*) cell through the relationship: $a_m \approx a_h$, $b_m \approx \sqrt{3} b_h$, $c_m \approx c_h$. The cell dimensions reported were obtained by a simplex refinement that minimized the differences in 2θ for 25 lines over the 2θ interval 19–47°. The estimated error in the cell dimensions is ±0.1%.

Thermogravimetric analysis by reduction in H_2/Ar (15:85) at 700°C gave $SrIrO_{3.0}$ for a ratio Sr:Ir = 1. It was noted that up to 400°C, the reduction proceeded according to the following reaction:

$$2H_2 + 2SrIrO_3 \rightarrow Sr_2IrO_4 + Ir + 2H_2O.$$

This intermediate step indicates that Ir^{4+} is more stable to reduction in the K_2NiF_4 structure of Sr_2IrO_4, where the higher Sr:Ir ratio provides a more oxidizing medium. The density of a batch of small crystals (~0.1 mm on edge) grown from a $SrCl_2$ flux was determined using the pycnometric method with water. The sample was outgassed by boiling at reduced pressure. The density found by averaging five separate determinations was 7.6 ± 0.1 g/cc and is to be compared to the theoretical density 7.57 g/cc.

Qualitative examination of the observed intensities indicated that the atomic arrangement for $SrIrO_3$ was essentially a distortion of the hexagonal form of $BaTiO_3$ (*2*) or the atmospheric pressure form of $CsMnF_3$ (*3*).

This hexagonal structure can be described as close-packed SrO_3 layers stacked perpendicular to the *c* axis in the sequence *hcchcc*, where *h* and *c* refer to hexagonal and cubic stacking, the Ir occupying the all-oxygen octahedra formed by the layers. These octahedra share common corners across a *c* layer and common faces across an *h* layer, giving pairs of face-shared octahedra that are joined by common corners to a plane of corner-sharing octahedra. This arrangement, together with

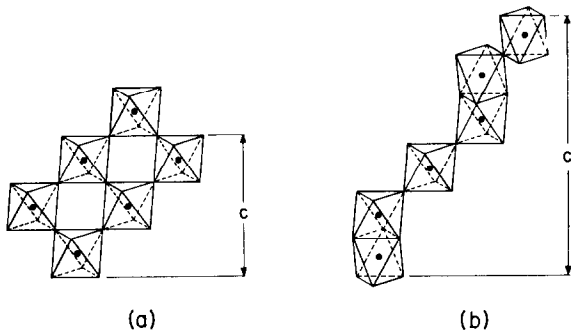

FIG. 1. Octahedra linkage for (a) perovskite structure and (b) hexagonal 6H structure.

* This work was sponsored by the Department of the Air Force.

† Current Address: Esso Research and Engineering, Box 45, Linden, N.J. 07036.

‡ Current address: Division of Engineering, Brown University, Providence, R.I. 02912.

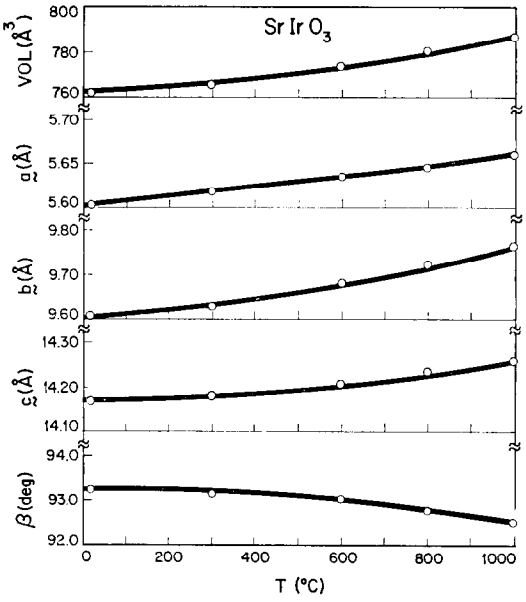

FIG. 2. Unit cell dimensions and volume as a function of temperature for the atmospheric-pressure form of $SrIrO_3$.

the all cubic-close-packed perovskite structure, is shown in Fig. 1. A detailed discussion of this structure and its relation to other close-packed ABX_3 compounds has been given by Katz and Ward (*4*).

If the monoclinic unit cell is a distortion of this six-layer hexagonal cell, then b/a should approach the ideal value of $\sqrt{3}$ as the temperature is raised. In studies of powdered samples using a General Electric XRD-5 with a Tempres high-temperature attachment, we have determined the lattice parameters to 1000°C. Figure 2 summarizes the data and shows the monoclinic cell becoming less distorted, approaching a hexagonal cell as $\beta \to 90°$ and $b/a \to \sqrt{3}(b/a = 1.716$ at room temperature and 1.726 at 1000°C). The thermal-expansion coefficient for the a axis is almost constant at $\alpha_a = 10 \times 10^{-6}/°C$. However, α_b and α_c increase with temperature from 8×10^{-6} to $22 \times 10^{-6}/°C$ for α_b and from 2×10^{-6} to $14 \times 10^{-6}/°C$ for α_c.

In order to test the proposed structure, integrated intensity measurements were made on the powder diffraction peaks by accumulating counts while slow-scanning ($\frac{1}{4}°$/min.) through a peak. The necessary background, as determined from a smooth curve measured where there were no nearby peaks, was subtracted. If two or more peaks overlapped appreciably, their intensity was treated as a single peak. A Norelco vertical diffractometer with monochromated (LiF crystal) CuK_α radiation was used to collect the data.

Atoms were placed in the positions of the monoclinic space group C 2/c (No. 15) as given in Table I. Due to the large number of position parameters for oxygen and its low scattering relative to Ir and Sr, it was decided to refine only the position parameters of Ir and Sr with the oxygens placed approximately as they are in $BaTiO_3$ (*2*). This was done using a computer program, written in our laboratory, that uses the simplex method to refine position parameters and cell temperature factor by minimizing the difference between observed and calculated intensities. Using intensity data to $2\theta = 64°$, the position parameters of Sr and Ir were refined to $R = \Sigma|I_o - I_c|/\Sigma I_o \approx 0.10$. Their values are listed in Table I. The position of the oxygens was determined by placing them around the cations in a

TABLE I

CRYSTAL STRUCTURE OF ATMOSPHERIC PRESSURE $SrIrO_3$

Space group	$C2/c$ (No. 15)
Unit cell dimensions	$a = 5.604$ Å, $b = 9.618$ Å, $c = 14.174$ Å, $\beta = 93.26°$ (±0.1%)
Cell contents	12 $SrIrO_3$ with $(\frac{1}{2},\frac{1}{2}, 0)$ translation for:
Sr_I in (4e)[a]	$\pm(0,y,\frac{1}{4})$; $y = 0.016(3)$
Sr_{II} in (8f)	$\pm(x,y,z; x,\bar{y},\frac{1}{2}+z)$; $x = 0.000(2)$, $y = 0.682(2)$, $z = 0.103(2)$
Ir_I in (4a)	(0,0,0; 0,0,$\frac{1}{2}$)
Ir_{II} in (8f)	$\pm(x,y,z; x,\bar{y},\frac{1}{2}+z)$; $x = 0.975(1)$, $y = 0.658(1)$, $z = 0.846(1)$
O_I in (4e)[b]	$\pm(0,y,\frac{1}{4})$; $y = 0.492$
O_{II} in (8f)	$\pm(x,y,z; x,\bar{y},\frac{1}{2}+z)$; $x = 0.224$, $y = 0.265$, $z = 0.260$
O_{III} in (8f)	$x = 0.770$, $y = 0.427$, $z = 0.083$
O_{IV} in (8f)	$x = 0.997$, $y = 0.170$, $z = 0.483$
O_V in (8f)	$x = 0.260$, $y = 0.415$, $z = 0.080$
Cell temperature factor: $B = 0.52$	

[a] Parameters for Sr and Ir positions determined by refinement.

[b] Parameters for O positions determined by bond distance considerations.

manner consistent with the structural chemistry of Sr and Ir. Table II compares all observed intensities to intensities calculated from the refined Sr and Ir positions and the most reasonable oxygen positions. The R factor based on all intensities is $R = 0.13$ and indicates that the structure of the atmospheric pressure form of $SrIrO_3$ is essentially a slight distortion of the hexagonal $BaTiO_3$ structure. A few selected bond distances are given in Table III.

The ideal hexagonal structure of $SrIrO_3$, designated (6H) according to polytype nomenclature (5), has two-thirds cubic close-packing and is one of a series of polytypes between the all hexagonal close packing of $CsNiCl_3$(2H) and the all cubic close

TABLE II

X-RAY DIFFRACTION DATA FOR ATMOSPHERIC PRESSURE $SrIrO_3$

($a = 5.604$ Å, $b = 9.618$ Å, $c = 14.174$ Å, $\beta = 93.65°$)

hkl	I_{calcd}	I_{obsd}	d_{obsd}	hkl	I_{calcd}	I_{obsd}	d_{obsd}
002	0.50	0.4[a]	7.08	042	0.59		
110	0.00	—[a]	—	20$\bar{4}$	0.81	2.5	2.26
020	0.01			222	0.29		
11$\bar{1}$	6.31	7.5	4.65	13$\bar{4}$	2.45	2.0	2.218
				22$\bar{3}$	0.01	—	—
021	14.18	24.6	4.53	11$\bar{6}$	0.01	—	—
111	11.49			134	1.21	1.0	2.158
11$\bar{2}$	5.80	2.9	4.09	043	2.26	2.0	2.140
022	4.02	4.8	3.98	204	0.00		
112	9.33	9.2	3.91				
004	0.69	1.8	3.54	026	0.01	1.6	2.111
11$\bar{3}$	0.43	0.2	3.46	223	1.66		
023	0.05	0.2	3.36	116	0.00	—	—
113	2.22	2.0	3.29	22$\bar{4}$	11.90	8.9	2.004
11$\bar{4}$	26.82	22.7[a]	2.926	13$\bar{5}$	0.10	—	—
024	17.99	23.2[a]	2.850	044	9.90	10.4	1.988
200	26.46	100.0[a]	2.788	135	0.03	9.7	1.953
114	20.16			224	8.75		
130	51.41						
				11$\bar{7}$	2.07	1.5	1.899
13$\bar{1}$	0.82	0.2[a]	2.748	22$\bar{5}$	4.78	4.3	1.886
131	1.12	0.3[a]	2.714				
20$\bar{2}$	0.64	0.2	2.656	027	2.08	3.6	1.86
13$\bar{2}$	0.24	0.2	2.617	20$\bar{6}$	1.52		
132	0.29	—	—	117	3.75		
202	.13	0.1	2.554	045	1.89		
11$\bar{5}$	4.28	4.9	2.497	310	0.02		
				31$\bar{1}$	0.06	9.2	1.83
025	6.42	6.4	2.438	13$\bar{6}$	1.86		
13$\bar{3}$	0.18			240	0.00		
				150	0.01		
220	0.00	—	—	24$\bar{1}$	0.26		
040	0.00	10.0	2.39				
22$\bar{1}$	0.39						
115	4.21						
041	0.95	2.6	2.36	15$\bar{1}$	0.57	7.5	1.797
133	0.04			311	1.18		
221	1.85			241	1.18		
006	1.12			151	1.40		
				31$\bar{2}$	0.20		
22$\bar{2}$	0.04	—	—	225	3.31		

TABLE II (continued)

hkl	I_{calcd}	I_{obsd}	d_{obsd}	*hkl*	I_{calcd}	I_{obsd}	d_{obsd}
$24\bar{2}$	0.40	7.1	1.77	331	0.29	6.0[a]	1.591
136	2.60			061	0.62		
$15\bar{2}$	0.42			314	3.02		
008	2.30			$22\bar{7}$	0.79		
				$33\bar{2}$	0.55		
206	2.32	5.3	1.75	$31\bar{5}$	1.40	1.8[a]	1.578
152	0.49						
242	1.73			062	0.02	1.4[a]	1.56
312	1.66			$24\bar{5}$	0.74		
				332	0.28		
$31\bar{3}$	0.10	—[a]	—				
$22\bar{6}$	0.08	—[a]	—	$33\bar{3}$	0.02	5.0[a]	1.54
$24\bar{3}$	0.00	—[a]	—	047	1.18		
$15\bar{3}$	0.28	—[a]	—	$15\bar{5}$	2.57		
				$20\bar{8}$	2.59		
$11\bar{8}$	0.70	1.3	1.688				
153	0.00			063	0.09	10.0[a]	1.513
046	0.35			155	2.25		
				$11\bar{9}$	2.04		
243	0.58	1.3	1.676	227	2.62		
313	1.02			$13\bar{8}$	2.67		
				245	0.65		
$31\bar{4}$	6.03	5.6	1.66				
028	0.57			333	0.00	2.6[a]	1.495
$13\bar{7}$	0.04	—	—	315	0.77		
				$33\bar{4}$	1.17		
226	0.00	4.5	1.646	029	0.65		
$22\bar{4}$	4.98			$31\bar{6}$	0.04	—	—
118	1.25	5.0	1.633				
$15\bar{4}$	4.43			119	0.92	2.8	1.474
				138	1.32		
137	0.05	11.0[a]	1.613	$24\bar{6}$	0.10		
330	10.09						
$33\bar{1}$	0.19			$22\bar{8}$	0.56	2.0	1.459
				064	0.11		
154	3.76	11.0[a]	1.600	208	0.64		
060	4.95			$15\bar{6}$	0.43		
244	2.68			334	0.02	—	—

[a] Not used in refinement of Sr and Ir atomic position because of errors associated with lines at low 2θ, because the lines are very strong and have too much influence on the refinement or the overlapping lines occurred over too large a 2θ span.

packing of perovskite (3C). It has been shown in every case studied, that high pressure favors cubic close packing for these ABX_3 polytypes. The 6H structures of $TlNiF_3$ (*6*), $CsFeF_3$ (*7*), $CsMnF_3$ (*7, 8*), $RbNiF_3$ (*8, 9*), and $RbMnCl_3$ (*10*), all transform to the perovskite structure at high pressure (7–80 kbar at 700°). A more complete discussion of the structural dependence of ABX_3 compounds on high pressure has been given by Syono, et al. (*8*), and Longo and Kafalas (*7, 11*).

If the structure of $SrIrO_3$ at atmospheric pressure is indeed a distortion of the 6H structure, then it should also transform under high pressure to the perovskite structure. Samples of $SrIrO_3$(6H) were tightly packed into cylindrical, gold, or platinum capsules with end plugs and subjected to high

TABLE III

SOME BOND DISTANCES (Å) FOR $SrIrO_3$ (Atmospheric Pressure Form)

Ir_{II}–Ir_{II}	2.75
Ir_I–6O	2×(1.99, 1.98, 2.02)
Ir_{II}–6O	(1.87, 1.89, 1.94, 1.96, 2.00, 2.04)
Sr_I–12O	2×(2.69, 2.78, 2.81, 2.87, 2.89, 3.01)
Sr_{II}–12O	2.57, 2.78, 2.92, 2.57, 2.78, 2.92, 2.64, 2.76, 2.81, 2.82, 2.84, 2.96
O–O (around Ir_{II})	2.52, 2.52, 2.51 (shared octahedral face between Ir_{II}–Ir_{II}), 2.78, 2.78, 2.90, 2.76, 2.75, 2.95, 2.98, 2.70, 2.72
O–O (around Ir_I)	2×(2.76, 2.79, 2.79, 2.86, 2.87, 2.87)
O–O (around Sr)	Range from 2.51–3.12

pressure (up to 65 kbar) in a belt apparatus before the temperature was raised. After ½ hr at temperatures up to 1700°C, all samples were quenched, followed by release of pressure.

The results of these high-pressure runs are summarized in Fig. 3, which shows that the 6H structure of $SrIrO_3$ transforms to the perovskite structure above 20 kbar at 1650°C and above 50 kbar at 700°C. The high-pressure perovskite phase ($a = 5.60$ Å, $b = 5.58$ Å, $c = 7.89$ Å) is slightly distorted to the *Pbnm* orthorhombic symmetry of $GdFeO_3$ or $SrRuO_3$. A comparison of observed and calculated intensities (based on the position parameters of $GdFeO_3$) (*12*) is given in Table IV. The position of

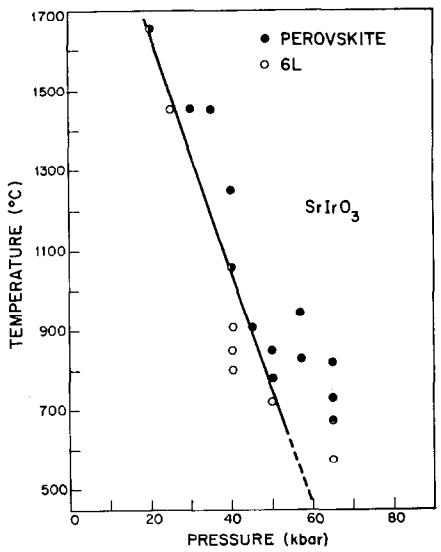

FIG. 3. Pressure–temperature diagram for the distorted 6H to perovskite transformation.

TABLE IV

CRYSTALLOGRAPHIC DATA FOR HIGH PRESSURE $SrIrO_3$ ($a = 5.60$ Å, $b = 5.58$ Å, $c = 7.89$ Å)

hkl	I_{obsd}	I_{calcd}
110, 002	S	24.3
111	W	2.3
020, 112, 200	VVS	100.0
021,	VVW	1.3
121, 211	VW	0.7
022, 202	W	2.8
113	VVW	1.0
122, 212	VVW	0.3
220, 004	S	27.1
221, 023,	VW	2.0
123, 213	VVW	0.4
130, 222, 310, 114	M	15.6
131, 311	VW	2.7
132, 024, 312, 204	VS	41.6
133, 313	VW	1.1
040, 224, 400	M	7.9
042, 330, 134 314, 402, 006	M	9.1
240, 332, 420, 116	S	15.6
242, 422, 026, 206	W	4.5
333, 135, 315	VW	1.6
044, 404	M	4.5
150, 334, 226, 510	W	4.5
152, 244, 136 424, 512, 316	M	18.4
440, 008	W	2.1
350, 154, 442, 046 530, 514, 118, 406	M	8.7
352, 532, 336 028, 600, 208	M	11.2
062, 246, 426, 602	W	4.1

the 021 reflection on a Guinier x-ray pattern taken and analyzed by Dr. A. W. Sleight of E.I. du Pont de Nemours and Company showed that $a > b$.

The perovskite (61.6 Å^3/molecule) represents a 3% reduction in volume from the 6H structure (63.5 Å^3/molecule). The quenched high-pressure phase is very stable at atmospheric pressure, only retransforming slowly to the 6H structure at 1200°C. This same stability was found for all the high-pressure polytypes in the system $Ba_{1-x}Sr_xRuO_3$ (*11*).

Electrical resistivity measurements on the perovskite phase were made using the four-probe Van der Pauw technique on a highly sintered disc. At 77°K, $\rho = 3 \times 10^{-3}$ Ω cm, and at 295°K, $\rho = 4 \times 10^{-3}$ Ω cm. The resistivity and its temperature dependence are similar to the metallic perovskite $SrRuO_3$. Rodi (*1*) has reported that the atmospheric pressure form of $SrIrO_3$ also has metallic conductivity.

Magnetic susceptibility measurements on a vibrating-sample magnetometer from 4.2–300°K in magnetic fields to 10kOe gave a temperature-independent $\chi_{1r} = 1.2 \times 10^{-3}$ emu/mole. Such a Pauli paramagnetism is also found for the atmospheric-pressure form of $SrIrO_3$ (*1*) and is consistent with the metallic conductivity of these materials.

At atmospheric pressure, $SrIrO_3$ and $SrMnO_3$ are the only $SrBO_3$ compounds (B = Ti, Zr, Hf, Cr, Mo, Tc, Fe, Ru, Sn, Pb, Ce, Th) that do not have the perovskite structure if B is able to accept octahedral coordination. $SrMnO_3$ has the 4H polytype structure with alternating cubic and hexagonal close-packed layers (*8*, *13*, *14*). It would appear that the hexagonal polytypes, with their face-shared octahedra and trigonal fields, are stabilized by outer-electron configurations that allow for metal–metal bonding along the *c* axis where the metal–metal distance is about 2.7 Å. This would suggest that the 2H polytype with all hexagonal-close-packed layers would be the stable structure. However, ion-size considerations would suggest the perovskite structure. Thus we see that the 6H-related structure of $SrIrO_3$ and the 4H structure of $SrMnO_2$ are compromises between the continuous face-shared chains of the 2H polytype and the more satisfactory bond distances offered by the perovskite structure. In $SrIrO_3$ it appears that the strontium ions distort the hexagonal cell in order to be better accommodated in the A site of this structure, which is larger than the A site of the perovskite.

Acknowledgments

We would like to thank J. B. Goodenough for many helpful discussions and gratefully acknowledge the technical assistance of D. A. Batson and C. H. Anderson.

References

1. F. Rodi, Dissertation, Eberhard-Karls-Universitat, Tulsingen, 1963.
2. R. D. Burbank and H. T. Evans, *Acta Crystallogr.* **1**, 330 (1948).
3. A. Zalkin, K. Lee, and D. Templeton, *J. Chem. Phys.* **37**, 697 (1962).
4. L. Katz and R. Ward, *Inorg. Chem*, **3**, 205 (1964).
5. A. R. Verma and P. Krishna, "Polymorphism and Polytypism in Crystals," J. Wiley and Sons, Inc., New York, 1966.
6. K. Kohn, R. Fukuda, and S. Iida, *J. Phys. Soc. Jap.* **22**, 333 (1967).
7. J. M. Longo and J. A. Kafalas, *J. Solid State Chem.* **1**, 103 (1969).
8. Y. Syono, S. Akimoto, and K. Kohn, *J. Phys. Soc. Jap.* **26**, 993 (1969).
9. J. A. Kafalas and J. M. Longo, *Mater. Res. Bull.* **3**, 501 (1968).
10. J. A. Kafalas, J. M. Longo, and D. Batson, "Solid State Research Report," vol. 2, Lincoln Laboratory, MIT, Lexington, Mass., 1970.
11. J. M. Longo and J. A. Kafalas, *Mater. Res. Bull.* **3**, 687 (1968).
12. S. Geller, *J. Chem. Phys.* **24**, 1236 (1956).
13. B. L. Chamberland, A. W. Sleight, and J. F. Weiher, *J. Solid State Chem.* **1**, 506 (1970).
14. T. Negas and R. S. Roth, *J. Solid State Chem.* **1**, 409 (1970).